Ising lattices with $\pm J$ second-nearest-neighbor interactions

A. J. Ramírez-Pastor and F. Nieto
Departamento de Física, Universidad Nacional de San Luis, CONICET, 5700 San Luis, Argentina

E. E. Vogel
Departamento de Ciencias Físicas, Universidad de La Frontera, Casilla 54-D, Temuco, Chile
(Received 3 October 1996; revised manuscript received 23 January 1997)

Second-nearest-neighbor interactions are added to the usual nearest-neighbor Ising Hamiltonian for square lattices in different ways. The starting point is a square lattice where half the nearest-neighbor interactions are ferromagnetic and the other half of the bonds are antiferromagnetic. Then, second-nearest-neighbor interactions can also be assigned randomly or in a variety of causal manners determined by the nearest-neighbor interactions. In the present paper we consider three causal and three random ways of assigning second-nearest-neighbor exchange interactions. Several ground-state properties are then calculated for each of these lattices: energy per bond ϵ_g, site correlation parameter p_g, maximal magnetization μ_g, and fraction of unfrustrated bonds h_g. A set of 500 samples is considered for each size N (number of spins) and array (way of distributing the N spins). The properties of the original lattices with only nearest-neighbor interactions are already known, which allows realizing the effect of the additional interactions. We also include cubic lattices to discuss the distinction between coordination number and dimensionality. Comparison with results for triangular and honeycomb lattices is done at specific points. [S0163-1829(97)08721-3]

I. INTRODUCTION

Ground state properties of Ising lattices with randomly distributed $\pm J$ exchange interactions (bonds) have been studied from different points of view.[1] Usually they consider first-neighbor or nearest-neighbor interactions (FNNI's) only. In the present paper we calculate and discuss ground-state properties of square lattices (SL's) where second-nearest-neighbor interactions (SNNI's) are added to the Hamiltonian, restricting ourselves to the case of equal magnitude and equal number of ferromagnetic and antiferromagnetic interactions.

The starting point is a previous work where 500 samples (bond distributions) were prepared for 43 different arrays of SL's with FNNI's, increasing size from 4 to 64 spins.[2] We use exactly those same individual lattices, defining SNNI's on them according to several different procedures to be defined below. On the other hand, 25 arrays with 500 samples each, were prepared in simple cubic lattices.

The work done so far on this kind of problem deals mostly or exclusively with FNNI's. On the other extreme, mean-field approaches are not suitable for the systems described above, where lack of homogeneity and local fields are extremely important. As a way to make progress toward a more realistic description of magnetic lattices with competing interactions we introduce here several ways of assigning SNNI's, calculate physical magnitudes and discuss the general trends.

Other important motivation for this work is related to the discussion concerning whether these lattices represent spin-glass behavior, with order parameters that do not vanish in the thermodynamic limit.[3] It has been shown that increasing the dimensionality such systems get closer to spin glasses.[4] When stepping from two to three dimensions the coordination number κ increases, but this can also be accomplished by extending the interactions to neighbors beyond the closest ones. Thus, for SL's we can go from $\kappa=4$ (when only FNNI's are considered) to $\kappa=8$ (when all SNNI's are present). For FNNI's in two dimensions it is usually accepted that a phase transition from a spin-glass phase to a nonordered magnetic state would occur at $T=0$.[5] Very recently, evidence has been provided indicating that such a phase transition could occur at $T>0$.[6] It is a legitimate question to ask whether SNNI's would help to stabilize such a spin glass phase.

If only half the SNNI's are present while the others are vacant, then κ is 6 as in simple cubic lattices in three dimensions. However, these two systems are not equivalent from the topological point of view and their results are quite different as shown in Sec. V. Then, by introducing interactions to distant neighbors we are proposing a new way of approaching the spin-glass behavior for $\pm J$ Ising lattices.

Another reason for the present work is to extend the characterization of the recently defined order parameters p_g and h_g, which have proven to be more drastic than previously defined parameters available in the literature.[7] Both quantities are state-oriented parameters that are complementary (and more computer demanding) than calculations focused on ground state energy and other related properties.[8,9] The microscopic approach used here can also be used to complement macroscopic treatments based on exact determination of the partition function.[10,11]

We also use this opportunity to study the shattered magnetization of these systems; this is an idea closely related to staggered magnetization in antiferromagnetic systems paying attention to the absolute value of the average magnetization $\langle \mu_g \rangle$ per site. It is known (and expected) that the total magnetization should average to 0.0 for fairly large systems.[1] However, some ground states may have surprisingly large shattered magnetizations, which backs the idea of a site or-

dering. The maximum absolute value of such magnetization will be called maximal magnetization of the ground state. Usually two (or an even number) of states will possess such maximal magnetization in opposite directions canceling each other when averaging over the ground manifold. However, if ergodicity is broken in such a way as to separate states with maximal magnetization, a net magnetization can remain in these systems as will be discussed below.

To calculate exactly the microscopic parameters p_g, μ_g, and h_g based on all the states in the ground manifold, we had to pay the price of restricting ourselves to small systems according to the computer facilities we can access. However, some general tendencies toward the thermodynamic limit can be obtained since the reported values are stable enough.

Section II defines the Hamiltonian and the magnitudes to be calculated and studied later. In Sec. III we present different ways of assigning SNNI's. Section IV presents the results for the properties for SL's under the different ways of defining SNNI's. Section V discusses such results comparing among the different possibilities of defining SNNI's. When possible, a comparison is made with results for simple lattices calculated here and also with previously reported results for triangular, square, and honeycomb lattices. At the same time several conclusions are obtained.

II. THEORY AND DEFINITIONS

The size of a lattice is the number of spins N. Each way of regularly distributing the N spins is called an array. We will consider distributions in two dimensions (SL's) and in three dimensions (simple cubic lattices). Spins interact by means of the well-known Ising Hamiltonian:

$$H=\sum_{i<j}^{N} J_{ij}S_iS_j, \tag{1}$$

where the sums extend over all pairs of nearest neighbors (square and simple cubic lattices) and second-nearest neighbors (SL's only), S_i and S_j represent the third component of the spins at sites i and j, respectively. The bond J_{ij} in between such a pair of spins can be either -1 energy unit (ferromagnetic or F) or $+1$ energy unit (antiferromagnetic or AF).

The original lattices used on a previous paper[2] (FNNI's only) were formed by randomly distributing these bonds through the lattice, half F and half AF. SNNI's will be specified in several manners, all preserving the condition of equal proportion of F and AF bonds. After bonds are allotted they remain fixed at their positions.

A state is represented by an ordered set of spin orientations. Here we are interested in the properties of the ground level of these systems, which is the reason to use index g to characterize the properties calculated and discussed below. Since the Hamiltonian of Eq. (1) is invariant under the simultaneous inversion of all spins, we need to consider half the configuration space only. Thus, W represents the degeneracy of the ground manifold for such space, while $2W$ would be the degeneracy in the complete configuration space.

A computer program has been designed based on partial enumeration of the configuration space. The idea is similar to the *branch and bound* algorithm[12,13] but the present method sets thresholds after considering rows rather than single spins. The ground manifold is obtained by finding the least energy E_g that also corresponds to the minimal frustration. It is more convenient to deal with the ground state energy per bond:

$$\epsilon_g=\frac{E_g}{B}, \tag{2}$$

where B is the total number of bonds in the lattice, which depends on the topology and the way to define the interactions to second-nearest neighbors. For example B is $2N$ for SL's with FNNI's only and it is $3N$ for simple cubic lattices. Generally speaking, in SL's we can write that

$$B=\frac{N\times\kappa}{2}. \tag{3}$$

The minimal circuit defined by bonds is called plaquette, which is said to be curved or frustrated when it is formed by an odd number of AF bonds. Otherwise the plaquette is said to be flat or unfrustrated. A theorem shows that the frustrated bonds in a ground state can be found when curved plaquettes are joined in pairs by means of *frustration segments*, which are defined as imaginary lines joining the centers of two curved plaquettes passing over frustrated bonds.[14,15] The total energy can be calculated by weighting all satisfied (frustrated) bonds with a negative (positive) unit of energy. We have made use of this theorem to check our computer programs based on enumeration of the low-energy portion of the configuration space. However, these technical aspects are omitted for reasons of space and continuity. The interested reader is kindly referred to the literature for details.[2,14–16]

The site order parameter p_g has been introduced[2] inspired by the previously defined $q(0)$ order parameter due to Edwards and Anderson.[17] Its expression is

$$p_g=\frac{1}{N}\sum_{i=1}^{N}\left|\sum_{\alpha} S_i^{\alpha}\right| \underline{\text{div}}\ W, \tag{4}$$

where α is an index that runs over the W ground states. Symbol $|\ |$ represents the absolute value of the variable and $\underline{\text{div}}$ means integer division.

The magnetization μ_g per site (or shattered magnetization) can be calculated by means of

$$\mu_g=\frac{1}{NW}\sum_{i=1}^{N}\left|\sum_{\alpha} S_i^{\alpha}\right|. \tag{5}$$

A major inconvenience concerning p_g [or $q(0)$] and μ_g is that they are strongly dependent on the ergodic breaking of the configuration space. In the present paper we calculate them by determining in a first run the largest region or island formed by bonds that do not frustrate in any of the states of the ground manifold. In a second run, the spins of this region free of frustration are obtained in a deterministic unique way, while all the others are let free to flip, using the algorithm mentioned above.

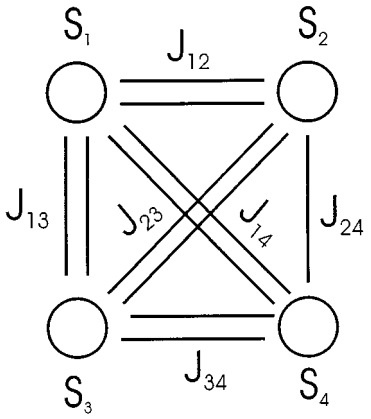

FIG. 1. Notation for first-nearest-neighbor interactions (FNNI's) and second-nearest-neighbor interactions (SNNI's) in one of the 16 possible square plaquettes. Spin at site i is denoted by S_i. FNNI's lie along the sides of the square, while SNNI's take place along the diagonals of the square.

Parameter h_g represents the fraction of bonds that never frustrate when scanning the entire ground manifold.[2] The corresponding expression is

$$h_g=\frac{1}{2N}\sum_{i<j}^{N}\left[\sum_{\alpha}^{W}\frac{|S_i^{\alpha}S_j^{\alpha}-J_{ij}|}{2}\right]\underline{\text{div}}\ W, \tag{6}$$

This parameter does not depend on the manner in which ergodicity is broken. Among its very interesting properties we can mention the values close to 0.50, 0.50, and 0.75 for triangular, square, and honeycomb lattices, respectively. Moreover, these three values remain constant independent of size and shape.[2,7,18–21]

If we remove from the original lattice all bonds that frustrate in any of the ground states we get a diluted lattice formed only by bonds that never frustrate. The ratio of the number of bonds in the diluted lattice to the number of bonds in the original lattice is precisely h_g. It has been recently shown that the diluted lattices present a typical percolation curve with respect to h_g as independent variable.[22] Other characteristics of this percolation are presently under study and will be published later on.

III. SECOND-NEAREST-NEIGHBOR INTERACTIONS

Almost all of the papers written on the lattices that concern us in the present study simply ignore long range interactions. On the other extreme, mean-field approximations are not suitable for systems where local fields are nontrivial. The introduction of SNNI's is one step further in the direction of describing more realistic systems, where intermediate range interactions play some role.

In square lattices, SNNI's occur naturally along the diagonal of the square cell or plaquette, as schematically presented in Fig. 1. The spin at site i is designated by S_i, the FNNI's are J_{12}, J_{24}, J_{34}, and J_{13}, while the SNNI's are denoted by J_{23} and J_{14} ($|J_{ij}|=1$ when different from zero).

The interactions to second-nearest neighbors can be thought as either independent or as a consequence of the nearest-neighbor interactions. In the first case we will speak of random assignment while in the second one we will say this is a causal assignment.

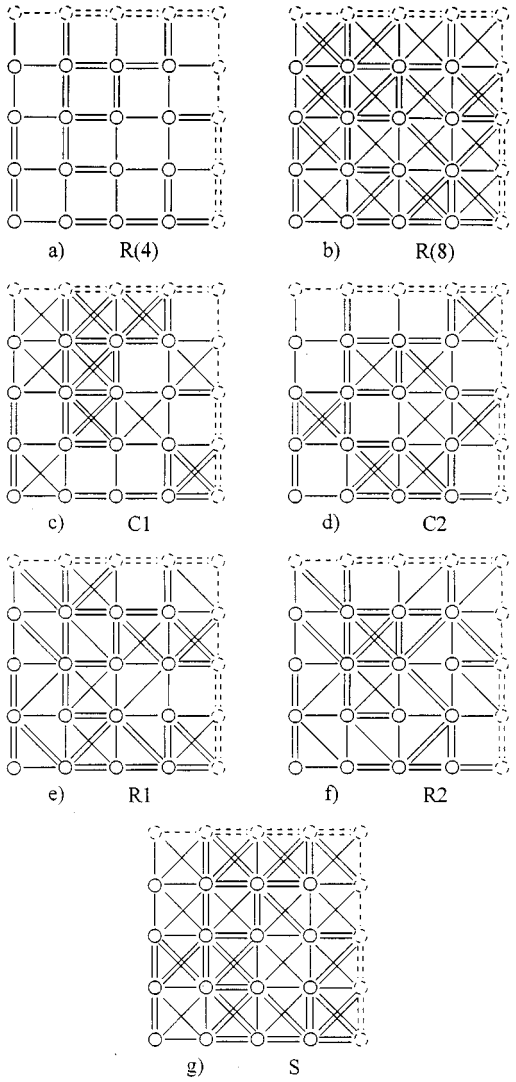

FIG. 2. (a) A particular 4×4 square lattice without SNNI's ($\kappa=4$). (b) All SNNI's are defined randomly with the constraint that the number of ferromagnetic interactions equals the number of antiferromagnetic interactions ($\kappa=8$). (c) Causal way $C1$ illustrated in Fig. 3 is applied to this example ($\kappa=6.5$). (d) Causal way $C2$ illustrated in Fig. 4 is applied to this example ($\kappa=6.0$). (e) Same number of SNNI's as in $C1$ but distributed at random ($\kappa=6.5$). (f) Same number of SNNI's as in $C2$ but distributed at random ($\kappa=6.0$). (g) Superposition of $C1$ to those cases where SNNI's defined by $C2$ vanish ($\kappa=8.0$).

The different situations are presented in Fig. 2, where we use the same symbols that will be introduced in the text to characterize different ways of assigning SNNI's. The concentration of SNNI's is different through the cases studied in Fig. 2, affecting average coordination number κ in a way that will be discussed below.

Random assignment: $R(\kappa)$. Here the SNNI's are assigned randomly in the same way as FNNI's. That is to say, the number of antiferromagnetic SNNI's is equal to the number of ferromagnetic SNNI's. However, the proportion in which SNNI's are present can be varied freely determining κ, which is an independent variable of interest in the present

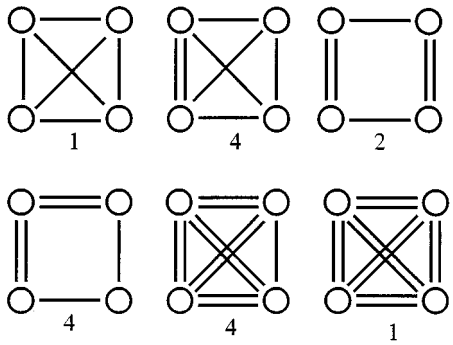

FIG. 3. Illustration of the way the causal way $C1$ works for each of the 16 plaquettes. FNNI's are previously defined along the sides of the square plaquette, while SNNI's arise along the diagonals of the square plaquette as defined in the text for $C1$. The multiplicity of each case is given underneath.

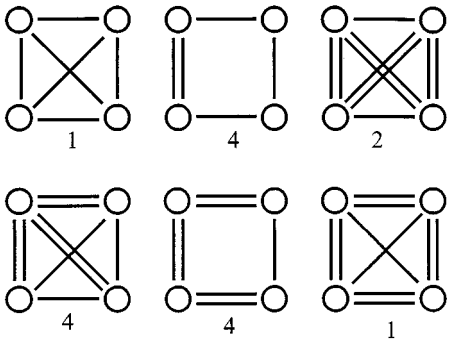

FIG. 4. Illustration of the way the causal way $C2$ works for each of the 16 plaquettes following the same presentation of Fig. 3.

work. This way of defining SNNI's is denoted by $R(\kappa)$. So $R(4)$ corresponds to the original SL where only FNNI's are present with coordination number 4, while $R(8)$ corresponds to the fully saturated lattice where all possible SNNI's have been defined randomly, with coordination number 8. Both extreme cases are presented on the top of Fig. 2.

Causal assignment. The general idea here is that FNNI's are a consequence of internal fields that automatically define all remaining interactions, in particular SNNI's. However, there is not a unique way in which this can happen. So we will now present two of such possibilities.

C1. In this procedure both SNNI's of a plaquette are given the same sign as most of the adjacent FNNI's. When there is no net majority, such SNNI's are taken to be vacant and they do not contribute to κ. This is illustrated in Fig. 3 for all possible plaquettes, while the application of the method to a particular example is realized in Fig. 2(c).

The signs of the nonvanishing SNNI's are obtained as follows:

$$\mathrm{sign}(J_{23}^{C1}) = \mathrm{sign}(J_{14}^{C1}) = \mathrm{sign}[J_{12}+J_{24}+J_{34}+J_{13}]. \tag{7}$$

When the sum vanishes, then $J_{23}^{C1} = J_{14}^{C1} = 0$, and such bonds are taken as nonexistent, so they are not considered in the calculations.

C2. There are always two paths connecting the same pair of second-nearest neighbors via two steps over first neighbors. In assignment $C2$, SNNI's are determined as to reinforce the effective interaction reached by simultaneously following these two paths. Namely, a diagonal interaction in the square plaquette is obtained as the normalized overlap of the two ways that connect the same points following the sides of the square. If these two ways lead to different results, the superposition yields a null result. This manner of defining SNNI's does not bring additional frustration to the system.

The mathematical expressions for this assignment are

$$J_{14}^{C2} = -\frac{(J_{12}\times J_{24}+J_{13}\times J_{34})}{2};$$

$$J_{23}^{C2} = -\frac{(J_{13}\times J_{12}+J_{34}\times J_{24})}{2}. \tag{8}$$

As in previous case, null bonds do not count. This is pictured for all plaquette configurations in Fig. 4, and it is applied to the example in Fig. 2(d).

Among the differences between $C1$ and $C2$ there is one that deserves special attention. If we make use of the multiplicity of the configurations given in Figs. 3 and 4 we realize that κ is different in these two cases. From the 16 possible plaquettes 10 have SNNI's for $C1$ (Fig. 3) and only 8 have them for $C2$ (Fig. 4). This essentially means that in the average

$$\kappa(C1) = 6.5, \quad \kappa(C2) = 6.0. \tag{9}$$

It follows that for an appropriate comparison it is convenient to define random concentrations for these values of average coordination numbers.

R1. It corresponds to allotting SNNI's in a random way with the constraint that the average value of κ is the same as in $C1$. Namely, $R(6.5) = R1$. This is illustrated in Fig. 2(e).

R2. It corresponds to assigning SNNI's in a random way, so to have $\kappa = 6.0$ as in $C2$. Namely, $R(6.0) = R2$, as illustrated in Fig. 2(f).

It follows from Figs. 3 and 4 that $C1$ and $C2$ coincide in assigning SNNI's for plaquettes with multiplicity 1, while they are complementary for all other plaquettes. That is to say, all SNNI's are different from zero invoking $C2$ first, then invoking $C1$ for those still nonexistent SNNI's. Then we can define a last causal way of realizing the interactions to second-nearest neighbors.

S. It is defined as the superposition of $C1$ to $C2$, whenever $C2$ fails to assign SNNI's. This is a saturated lattice, with $\kappa = 8.0$, so it can be compared to $R(8)$. This is presented in the last picture of Fig. 2.

Let us stress the fact that for each of the 500 samples, for a given array, in each size of SL's, we assign all SNNI's and then proceed to calculate the physical parameters. We verified that the distributions of the causal ways are centered at the expected values of κ.

It is also of interest to separate the roles of connectivity and dimensionality in these Ising lattices. Consequently we also prepared sets of 500 samples in three-dimensional arrays with cubic symmetry with FNNI's only. Notice that the coordination number is 6 for simple cubic lattices, the same as in $C2$ and $R2$. A modified algorithm was used that applies bounds to rows and planes.

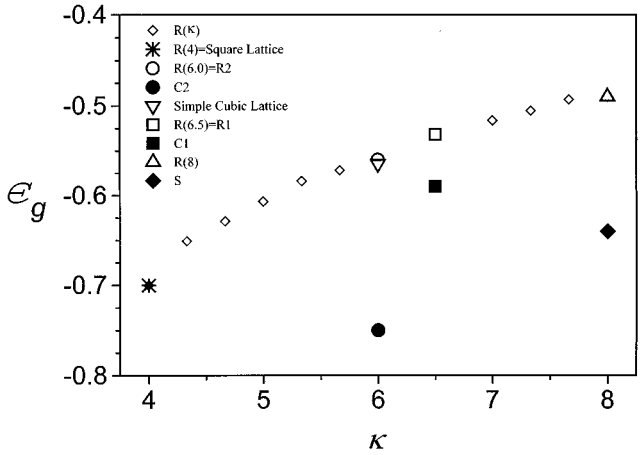

FIG. 5. Saturated values of ϵ_g for the random and causal ways of defining SNNI's presented in the text, corresponding to different coordination numbers κ. Additionally, sets of 500 random lattices were defined to cover the intermediate cases of κ.

IV. RESULTS

Results differ somewhat when going from one sample to another. We want to minimize fluctuation effects looking for correspondence of our results with those that are valid in the thermodynamic limit. All results to be reported below correspond to arithmetic averages for 500 samples for each array reported here.

The least sensitive parameter is ϵ_g, which saturates very fast with respect to size N. Although not shown here, we can say that the different curves ϵ_g vs N, corresponding to the different way of assigning SNNI's, are clearly stabilized for $N \geqslant 30$. Such size independent result will be called saturated value of the parameter. $C2$ exhibits the lowest ground-state energy at about -0.75. On the other extreme R has the highest value for $\epsilon_g = -0.49$.

The saturated values of ϵ_g as function of κ are presented in Fig. 5. The seven different assignments are denoted by symbols that will be used in the remaining illustrations. In addition to the seven lattices defined in Fig. 2, we prepared samples with random assignments of SNNI's to cover the interval $4.0 \leqslant \kappa \leqslant 8.0$. The corresponding saturated average values are represented by diamonds in Fig. 5, showing that the cases of random assignment lay along a concave curve containing all $R(\kappa)$ points. Evidently the causal SNNI's show lower values of ϵ_g than the corresponding values for random assignments. In particular $C2$ leads to the lowest value of ϵ_g among all the cases reported in the present work. A remarkable fact is that the cubic lattices show a saturation value intermediate as compared to those of some random ways of assigning SNNI's in two dimensions.

The results of p_g as functions of size N are presented in Fig. 6 for six different ways of assigning SNNI's. The causal ways show higher values and lower rate of decrease for two dimensions. The cubic case presents an apparently saturated value for p_g at 0.6. Anyhow, it is important to remember that the value and tendency of this parameter are determined by the way the ergodic separation is done. The present calculations made use of the ergodic separation given by the largest region that is free of frustration if the ground level as mentioned above.

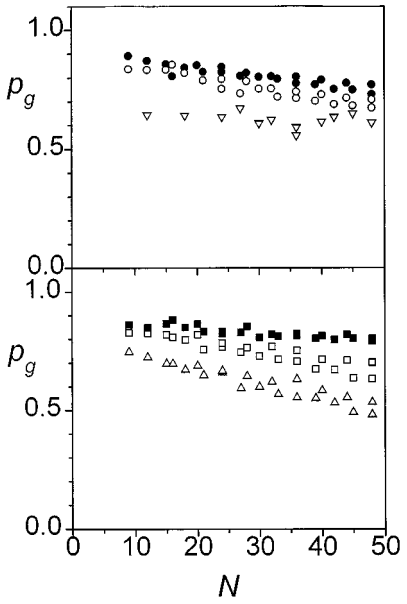

FIG. 6. Site correlation parameter p_g as function of N for six different lattices defined in the text. While the two-dimensional lattices decrease with different slopes as functions of size N, the cubic lattice shows a saturated value for p_g.

The results for maximal shattered magnetization per sample corresponding to 6×6 lattices with causal SNNI's assignments are presented in the forms of histograms in Fig. 7. Average values over the 500 samples are given in the insert. $C1$ presents a more extended distribution than $C2$. The remarkable fact is that for all distributions a net magnetization remains in the lattices. One could say that at least three spins out of five point in one direction while the remaining two spins point in opposite direction. This observation is valid for the ergodic separation mentioned before.

The results for the fraction of nonfrustrated bonds h_g are presented in Fig. 8. The tendencies of the results for each way of assigning SNNI's do not show size dependence so

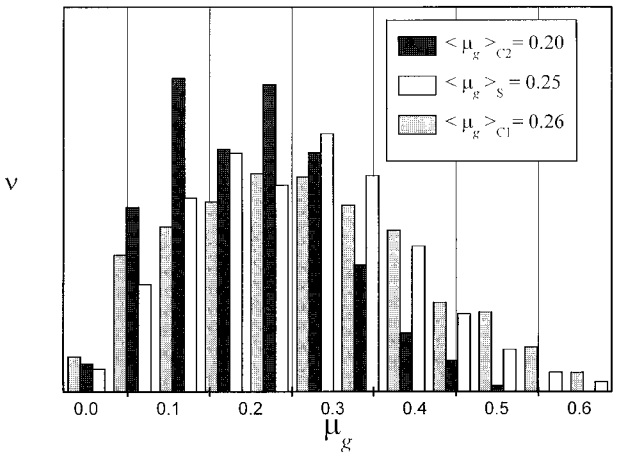

FIG. 7. Histograms showing the prevalence of shattered magnetization in the ground states of 6×6 lattices with causal ways of defining SNNI's. For each of the 500 samples the maximal shattered magnetization is found. The height of the histogram ν represents the number of samples with maximal shattered magnetization in the corresponding interval.

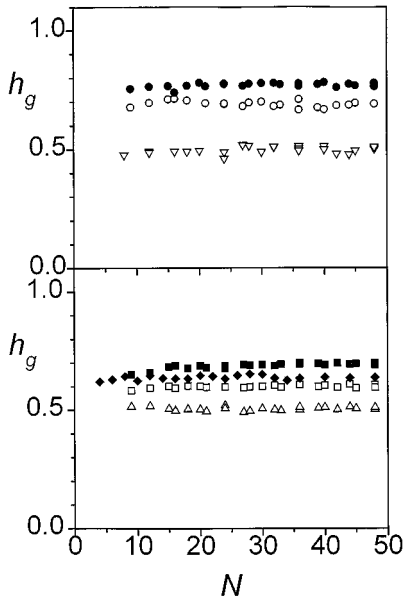

FIG. 8. Parameter h_g representing the fraction of the lattice that remains free of frustration for the entire ground manifold as functions of N. For the seven different lattices this variable is essentially size independent.

they are already saturated for small samples. The causal ways give higher values for h_g being $C2$ the one that gives the highest value close to 0.77. It is interesting to remember that h_g is independent of ergodic separation.

V. DISCUSSION AND CONCLUSIONS

Generally speaking the random increase of the coordination number κ leads to an increase in the energy per bond ϵ_g. It also affects the site correlation parameter p_g, the maximal shattered magnetization μ_g and fraction of nonfrustrated bonds h_g. However, for these last three parameters the dependence is not direct as other characteristics such as geometry and topology play important roles.

Frustration can be diminished to some extent when SNNI's are determined causally by FNNI's in a way that can be optimized. A way to do this is $C2$, where SNNI's are to be chosen so they reinforce the action of FNNI's. Then the ground-state energy is lower and h_g increases. These comments apply in a moderated way for the case of $C1$.

The energy per bond saturates very quickly with size no matter which way of assigning SNNI's is chosen. The results for square lattices with $R2$ and simple cubic lattices are basically the same. This shows that energy does not discriminate whether the coordination number comes via dimensionality or via SNNI's, as far as these interactions are assigned randomly.

As for the site correlation parameter p_g, both $C1$ and $C2$ yield an increase in the values. Even better, such higher values decrease in a moderate way as N increases. It is not clear from the results of the small samples that we could process until now, whether p_g will go to zero in the thermodynamic limit. This argument is backed by the size independence of p_g for cubic lattices as presented in Fig. 6.

From the results presented above it follows that site correlation parameter p_g does not show saturation for any of the ways of assigning SNNI's. Larger lattices should be used before drawing any firm conclusion in this respect. Values for $C1$ and $C2$ are not notoriously different, although the tendency is that $C1$ leads to slightly more size independent results. On the other hand, the results for cubic lattices showing a behavior close to a saturated value for p_g, tells that this parameter is more sensitive to dimensionality than to coordination number.

TABLE I. Saturated values of h_g for the seven lattices defined in Fig. 2 plus three other two-dimensional lattices informed in the literature. Hexagonal: Ref. 15; square: Ref. 2; triangular: Ref. 2. The coordination number κ for each lattice is given in the second column.

Lattice	κ	h_g
Hexagonal	3	0.75
Square	4	0.50
Triangular	6	0.50
Cubic	6	0.50
$R2$	6	0.70
$C2$	6	0.79
$R1$	6.5	0.60
$C1$	6.5	0.70
R	8	0.50
S	8	0.64

The $\pm J$ Ising lattices with SNNI's defined in an optimized causal way are still candidates for a spin-glass behavior. At least the site order parameter p_g shows a more stable value in these modified lattices than in the usual random lattices with FNNI's only. It would be interesting to extend the present analysis to increase both dimensionality and range of the interactions. An immediate example are cubic lattices with SNNI's added in a causal optimized way.

The ergodic separation done here considered fixing the spins in the largest region free of frustration. From all the ground states, it is possible to isolate those states that provide the largest net magnetization in the lattice leading to the maximal shattered magnetization. This can be realized in real systems by means of a strong magnetic field applied during quenching. States with maximal magnetization are always present in the systems under study as shown by their spectral distributions presented in Fig. 7. $C2$ shows a more homogeneous response based on narrower maximal magnetization distribution as compared to $C1$. Different values are obtained for this magnitude when different ways of breaking ergodicity are utilized. We have defined a definite way of carrying on this process that leads to this relatively high value of shattered maximal magnetization. At the moment we cannot say if this is an artifact of the small sizes of the samples used here.

The fraction of nonfrustrated bonds is a very interesting parameter in many respects. No matter which way of assigning SNNI's is chosen, h_g saturates rather quickly with size. There is a clear discrimination between causal and random mechanisms of assigning SNNI's as the former shows larger values for this parameter. A summary of the properties of this parameter is given in Table I. The causal ways are clearly different: $C2$ presents less frustration than $C1$. The upper part of Fig. 8 shows that there is a drastic discrimina-

tion among lattices with the same $\kappa=6$: The cubic lattices present more frustration than SL's with similar connectivity. Actually causal ways of assigning SNNI's do not always reduce frustration: Fig. 8 clearly shows that saturated values for h_g are larger for $R2$ than for $C1$ or S.

In a cubic lattice any bond is shared by four square plaquettes, any of which can frustrate. On the other hand, in a SL with $C2$ any bond is shared by two square plaquettes and either 0, 2, or 4 triangular plaquettes. However, due to the way of constructing $C2$, none of the triangular plaquettes can be curved so the chances of frustrating the common bond are due to the two adjacent SL's only.

In this way $C2$ is built as to increase the connectivity in the lattice without bringing in more frustration. The original frustration remains local while it is diluted in several possible interactions, decreasing ϵ_g and increasing h_g. This is not so for $C1$ where half the triangular lattices brought in by SNNI's frustrate. We notice that the latter happen only inside frustrated square plaquettes while the random assignment $R1$ can take place in any square plaquette thus spreading frustration through the lattice.

ACKNOWLEDGMENTS

The first two authors were partially funded by CONICET, Fundación Antorchas (Argentina) and the European Economic Community through project ITDC-240. The last author was partially supported by FONDECYT (Chile) under Contract No. 1960972, and Dirección de Investigación y Desarrollo (Universidad de La Frontera) under Contract No. 9408. The three authors thank Instituto de Verano de Fisica of Universidad Austral de Chile for providing the opportunity to begin this collaboration.

[1] K. Binder and A. P. Young, Rev. Mod. Phys. **58**, 801 (1986).
[2] E. E. Vogel, J. Cartes, S. Contreras, W. Lebrecht, and J. Villegas, Phys. Rev. B **49**, 6018 (1994).
[3] I. Morgenstern, Phys. Rev. B **25**, 6071 (1982).
[4] R. N. Bhatt and A. P. Young, in *Heidelberg Colloquium on Glassy Dynamics, Proceedings, Heidelberg, 1986,* edited by J. L. Hemmen and I. Morgenstern, Lecture Notes in Physics Vol. 275 (Springer-Verlag, Heidelberg, 1986).
[5] I. Morgenstern and K. Binder, Phys. Rev. B **22**, 288 (1980).
[6] T. Shirakura and F. Matsubara, J. Phys. Soc. Jpn. **64**, 2338 (1995).
[7] E. E. Vogel, S. Contreras, W. Lebrecht, and J. Cartes, J. Magn. Magn. Mater. **140-144**, 1793 (1995).
[8] H. Freund and Peter Grassberger, J. Phys. A **22**, 4045 (1989).
[9] J. A. Blackman and J. Poulter, Phys. Rev. B **44**, 4374 (1991).
[10] L. Saul and M. Kardar, Phys. Rev. E **48**, R3221 (1993).
[11] L. Saul and M. Kardar, Nucl. Phys. B **432**, 641 (1994).
[12] H. A. Taha, *Integer Programming* (Academic, New York, 1965).
[13] S. Kobe and A. Hartwig, Comput. Phys. Commun. **16**, 1 (1978).
[14] G. Toulouse, Commun. Phys. **2**, 115 (1977).
[15] J. Vannimenus and G. Toulouse, J. Phys. C **10**, 537 (1977).
[16] F. Barahona, R. Maynard, R. Rammal, and J. P. Uhry, J. Phys. A **15**, 673 (1982).
[17] S. F. Edwards and P. W. Anderson, J. Phys. F **5**, 965 (1975).
[18] A. J. Ramírez, Magister thesis, Universidad Austral de Chile, Valdivia, 1996.
[19] F. Nieto, Magister thesis, Universidad Austral de Chile, Valdivia, 1996.
[20] E. E. Vogel and W. Lebrecht, Z. Phys. B **102**, 145 (1997).
[21] W. Lebrecht and E. E. Vogel, in *Magnetism, Magnetic Materials and their Applications*, edited by F. Leccabue and V. Sagredo (World Scientific, Singapore, 1996), p. 304.
[22] E. E. Vogel, S. Contreras, J. Cartes, and M. A. Osorio, in *Magnetism, Magnetic Materials and their Applications* (Ref. 21), p. 152.